RESEARCH PAPER

CrossMark

A novel method for fatigue assessment of steel plates with thermally cut edges

J. Peippo[1] · T. Björk[2] · T. Nykänen[2]

Abstract

The fatigue strength of thermally cut edges shares many similar features with the fatigue strength of a welded joint. Current design standards are valid for geometrically simple, straight, flame-cut edges made of mild steel. However, the applicability of current recommendations is questionable if the geometry is more complicated, if a different (thermal) cutting process is employed, or if any high-strength steel is used. In this study, conventional fatigue analysis methods are applied in order to explain the experimental results obtained by conducting fatigue tests on a cut component made of different steel grades. Since those methods did not explain the experimental results properly, a novel fatigue analysis method for plates with a thermally cut edge was created. This method is a parallel approach to that recently developed at Lappeenranta University of Technology for analyzing fatigue of a welded joint. In addition to the general stress range, this method also takes into account the structural and local geometry of the cut detail, surface roughness, residual stresses due to the cutting process, the external stress ratio, and the effect of the steel grade. The method agreed well with the test results and can be recommended as a new general approach for analyzing the fatigue of cut edges.

Keywords Fatigue strength · Cut edges · Design methods · Fatigue parameters · Surface roughness · Residual stress · Steel grades

1 Introduction

The current design codes and standards obtain fatigue design information for cut edges as fatigue strength at 2 million cycles (FAT) classes, and the method is similar to analyzing welded joints [1–4]. However, values are available in these for straight edges, while there are no recommendations for how curved edges with stress concentrations should be calculated. In some, design codes consider both the quality of the cutting process and the steel grade, but not the effect of residual stresses caused by cutting and the mean value of the applied load. The recommendations do not take the methods into account, and the same rules are applied for all thermal cutting processes.

This study takes the curved shape of the cut edge into account by using the local stress due to the structural shape as a nominal stress for fatigue analysis. The effect of the quality of the cutting process is taken into account as surface roughness, while the effective stress range is defined by considering also the residual stresses and mean stress in addition to the applied stress range. Based on this information, a new approach is created for analyzing the fatigue of cut edges, and the method is compared with experimental results.

The research is based on a practical case to try to fix the quality of the thermal cutting process for some components of a lifting device used by Konecranes Corporation, a large multinational company. Consequently, the quality had to be controlled using just a minimum number of parameters and using insofar as possible just nominal values. This posed some challenges for analyzing the experimental results, because more information about the properties of test specimens would ideally be available. However, this minimized information enables different suppliers all around the world control the quality of their manufacturing.

The goal of this study is to develop a novel method for the fatigue analysis of thermally cut edges that includes stress concentration and that takes into account, in addition to the stress range, also residual stress, mean stress, the steel grade,

---

Recommended for publication by Commission XIII - Fatigue of Welded Components and Structures

✉ J. Peippo
  juha.peippo@konecranes.com

1 Konecranes Global Oy, P.O. Box 661, FIN-05801 Hyvinkää, Finland

2 Laboratory of Steel Structures, Lappeenranta University of Technology, P.O. Box 20, FIN-53851 Lappeenranta, Finland

and the quality of the cutting process. The paper is based on doctoral dissertation work carried out by Juha Peippo [5].

2 Materials and methods

2.1 Materials

The research included structural steel grades S235, S355, and S960. All of these selected steels are weldable and can be cut by all thermal workshop processes. As mentioned in the previous chapter, the materials were characterized only by their nominal values. The chemical compositions of the steels used are seen in Table 1 and their mechanical strength in Table 2.

2.2 Experimental tests

The laboratory tests were carried out using a standard component for a crane lifting device. The test specimen is illustrated in Fig. 1.

The cutting methods applied were laser and plasma, but some reference specimens were prepared also by machining. A few test specimens were also heat-treated in order to affect the residual stresses.

The symmetrical specimens are load-carrying components, where the lower corners of the rectangular inner hole are the critical areas due to the applied load (see Fig. 6b). Consequently, the real radius, residual stresses, hardness distribution, and surface roughness were measured in those corners. The mean values of the dependence of the measured corner radius on the fabrication process are illustrated in Fig. 2.

The tangential residual stresses in the corner area were measured using the X-ray method. Since it was not possible to measure the stresses on the cut surfaces in the corner, they were measured on the plate surface as illustrated in Fig. 3.

The hardness values were measured as illustrated in Fig. 4a, and the measured distributions for the cutting processes applied and the material are shown in Fig. 4b–d.

Since also the surface roughness was impossible to measure in the corner itself, the flat surface of the rectangular hole was used as the reference surface. The results are illustrated in Fig. 5.

Table 1 Nominal values of chemical compositions of materials used. [%]

Steel	C	Si	Mn	P	S	N	Cu	Ti
S235J2G3	0.19	–	1.50	0.035	0.035	–	0.60	–
S355J2G3	0.23	0.60	1.70	0.035	0.035	–	0.60	–
S960QC	0.11	0.25	1.20	0.029	0.010	–	–	0.070

Table 2 Nominal strength values for materials used

Steel	f_y	f_u	A_5	E
S235J2G3	235 MPa	340–470 MPa	24%	207,000 MPa
S355J2G3	345 MPa	490–630 MPa	19%	207,000 MPa
S960QC	960 MPa	1000 MPa	7%	207,000 MPa

The test set-up is shown in Fig. 6a, and the local loading of the specimen is illustrated schematically in Fig. 6b. A constant amplitude loading was applied using different mean stress values and thus different R-values as seen in Table 3.

2.3 Finite element analyses

Finite element analyses were performed to define the stress concentration in the corner of a test sample at the point of the applied loading. As presented in Fig. 2, the scatter of radius values is quite large and this in consequence has an effect on the stress concentration and fatigue strength. Closer investigation of the corners proves that the plasma cut produces typically larger local radiuses than the laser process, as illustrated in Fig. 7a–d. Schematic versions of these local radiuses are shown in Fig. 7e–f.

Figure 8a shows the finite element analysis (FEA) model used, including the contact between the wedge and the specimen. Figure 8b shows the elastic stress concentration factor K_t depending on the corner radius. Peterson [6] equations match the FEA results very well.

However, if the real macro-level cutting shape (see Fig. 7) is considered also in the FEA model, as illustrated in Fig. 9, the local stress concentration is much higher than that presented in Fig. 8. The stress concentration on the cut surface is more
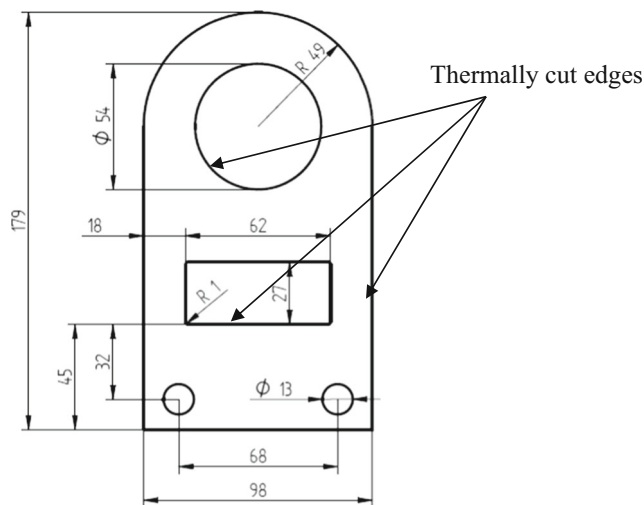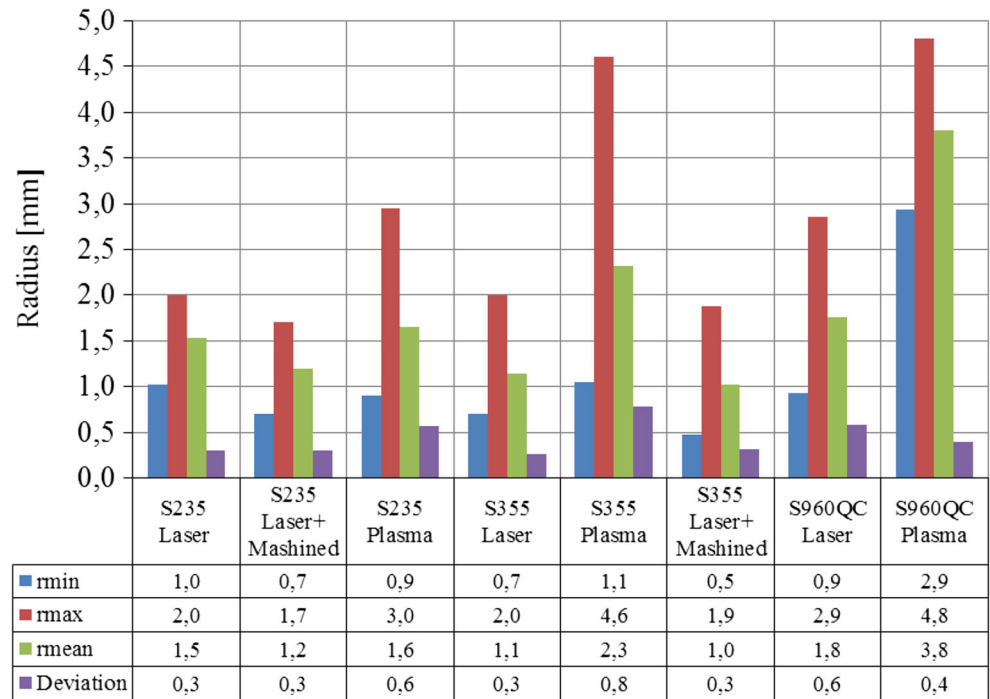

Fig. 1 Test specimen. The plate thickness was 10 mm for S235 and S355 samples and 8 mm for S960QC samples, respectively

Fig. 2 Measured average corner radiuses

	S235 Laser	S235 Laser+ Mashined	S235 Plasma	S355 Laser	S355 Plasma	S355 Laser+ Mashined	S960QC Laser	S960QC Plasma
■ rmin	1,0	0,7	0,9	0,7	1,1	0,5	0,9	2,9
■ rmax	2,0	1,7	3,0	2,0	4,6	1,9	2,9	4,8
■ rmean	1,5	1,2	1,6	1,1	2,3	1,0	1,8	3,8
■ Deviation	0,3	0,3	0,6	0,3	0,8	0,3	0,6	0,4

or less fractal, and the scaling level must be considered a reference FAT class.

FEA were exploited also to define the stress values for the following approaches: structural stress (hot spot), effective notch stress (ENS), local strain, and linear-elastic fracture mechanics (LEFM). Figure 10 shows the definition principle for hot spot stress and fatigue life based on LEFM, calculated by means of FRANK 2D-program.

2.4 Conventional analysis methods

Conventional analysis methods can be divided into two different main groups: the global (nominal) and the local methods. These methods are based on the stress, strain, or stress intensity factor. The basic assumption in several

standards and guidelines is that material strength does not affect fatigue resistance, as has been presented in Fig. 11. The exception is EN 13001-3 Cranes–General Design [2], wherein the fatigue classes of thermally cut edges are a function of yield strength, as shown in Fig. 11.

In this study, the nominal stress approach was applied, based on the stress in the corner. By using the linear stress concentration factor K_t and an effective stress range that considered the stress ratio R, the fatigue class FAT could be defined based on the fatigue test result N_f and nominal stress range $\Delta\sigma$. The slope m was fixed, according to current recommendations, at 3.

$$\text{FAT} = \sqrt[m]{\frac{N_f}{2\cdot 10^6}}\cdot\sqrt{1-R}\cdot K_t\cdot\Delta\sigma \qquad (1)$$

Fig. 3 The measuring point and direction of residual stresses (**a**) and the values dependent on the steel grade and the cutting process
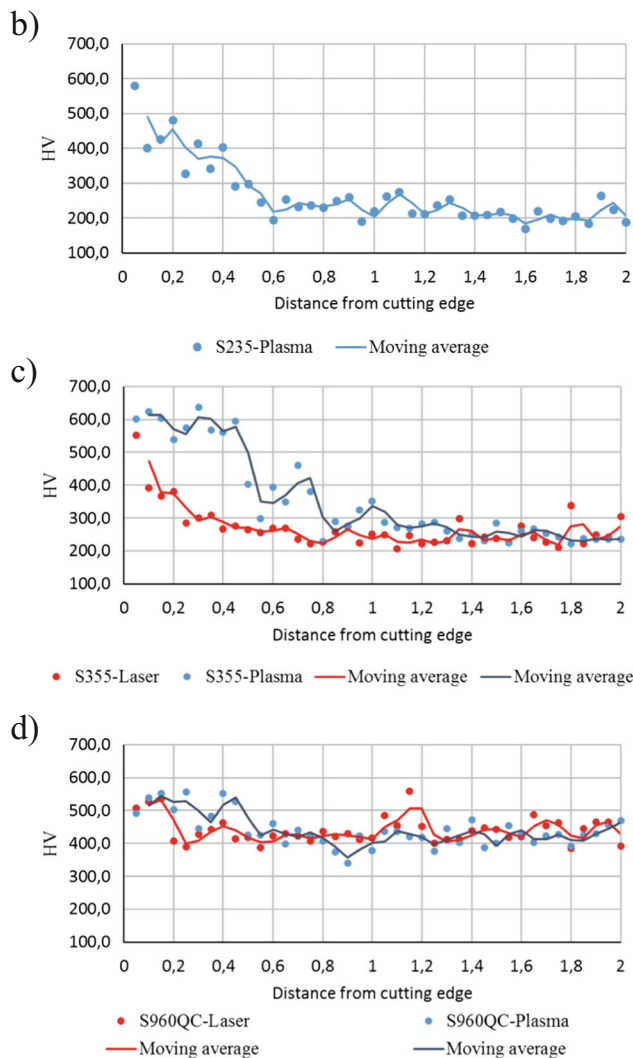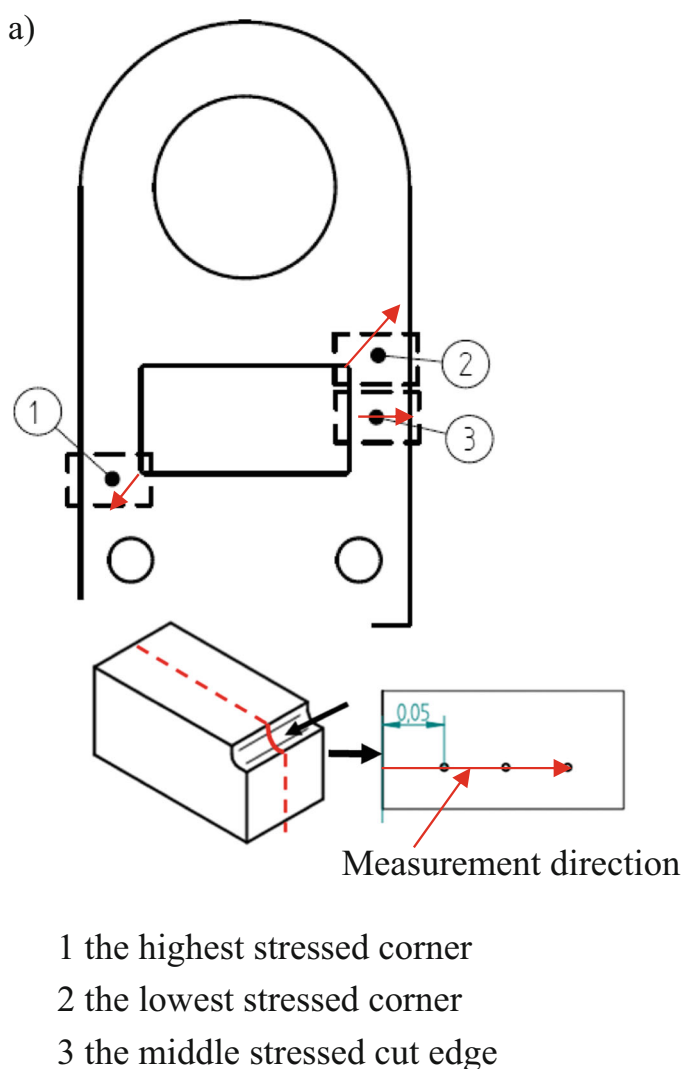

a) Location of measurement

a)

Measurement direction

1 the highest stressed corner

2 the lowest stressed corner

3 the middle stressed cut edge

b)

c)

d)
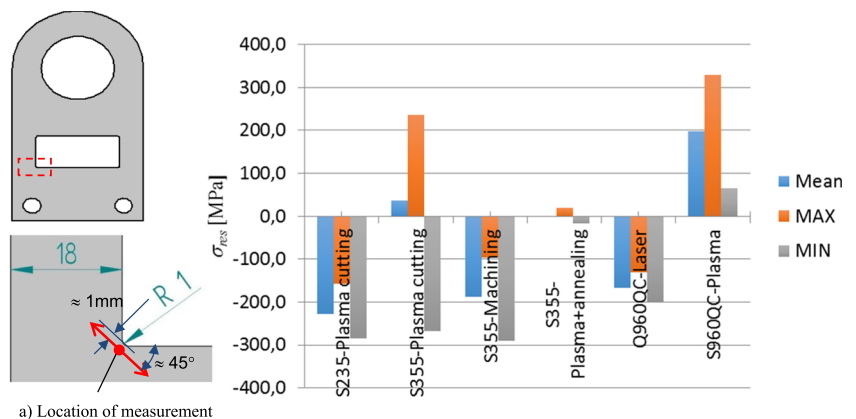
Fig. 4 Definition path for hardness distribution (**a**) and results from corner 1 for S235 (**b**), S355 (**c**), and 960 (**d**)

The true stress ratio parameter R_{true} is the local stress ratio depending on the stress range and ratio of an external load, the material strength, and residual stresses. The simple application based on the Neuber rule is illustrated in Fig. 12.

Structural hot spot stress, the effective notch stress method, strain-based methods, and fracture mechanics methods are all examples of local methods that can be used in fatigue analysis. These local methods are not very commonly used for estimating the fatigue strength of thermally cut edges. However, the hot spot method is applied here by defining the structural stress from the stress distribution along the line 1 in Fig. 10. Because of the high stress gradient in the critical ligament (line 1), the linear extrapolation is replaced with a more local stress approach. Thus, Eq. (1) can be applied just by replacing the $K_t \Delta \sigma$ value with the hot spot stress range.

The effective notch method is applied based on the measured corner radius instead of on the standard $r = 1$ mm

approach. The FAT classes can be obtained by applying Eq. (1), and the results will be mean values for ENS and thus, the reference FAT value is 308 MPa.
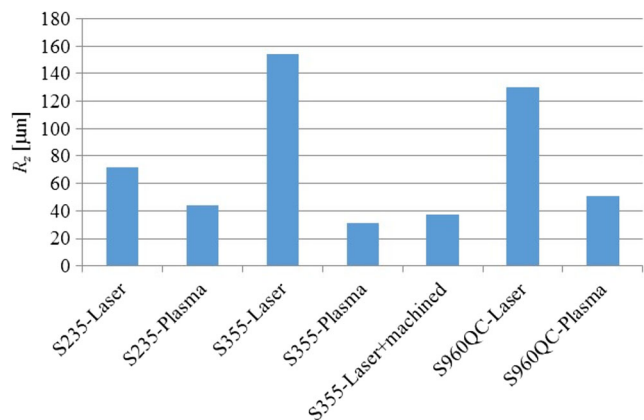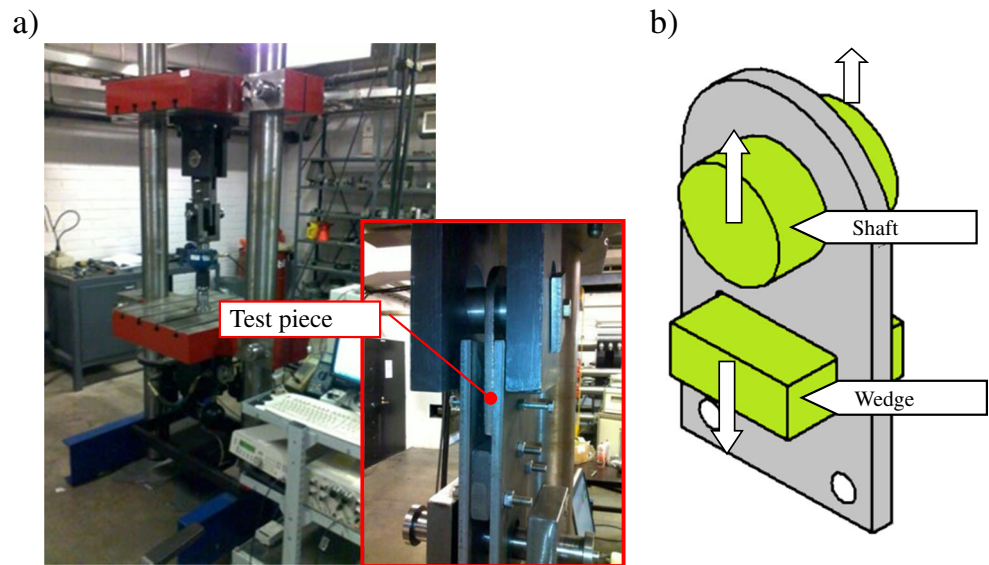

Fig. 5 Surface roughness depends on the materials and cutting methods

Fig. 6 Test set-up (**a**) and local loading of the specimen, schematically, (**b**)

a)

Test piece

b)

Shaft

Wedge

The local strain-based approach can be used to estimate the fatigue strength of the corner. Both the Smith, Watson and Topper (SWT) model presented in Eq. (2) and Morrow's model in Eq. (3), respectively, are applied.

$$\sigma_{\max}\cdot\frac{\Delta\varepsilon}{2}\cdot E = \left(\sigma_f'\right)^2\cdot\left(2\cdot N_f\right)^{2\cdot b} + \sigma_f'\cdot\varepsilon_f'\cdot E\cdot\left(2\cdot N_f\right)^{b+c} \quad (2)$$

$$\frac{\Delta\varepsilon}{2} = \frac{\sigma_f'-\sigma_{mt}}{E}\cdot\left(2\cdot N_f\right)^{b'} + \varepsilon_f'\cdot\left(2\cdot N_f\right)^{c'} \quad (3)$$

The material parameters required were defined based on hardness measurements [7]. The method obtains fatigue strength as the number of cycles, which can be changed back to FAT classes in order to facilitate comparison.

The number of cycles N_f obtained from Franc 2D analyses is used to calculate the LEFM-based FAT for the corner, as illustrated in Fig. 10.

2.5 New "FAT-mod" approach

A new approach called "FAT-mod" that takes into account all the essential fatigue parameters for thermally cut edges—such as the external stress range and ratio, residual stresses, the quality of the cut surface, and the strength of the material—was developed by Peippo in his doctoral dissertation [5]. The method is an important expansion of the similar type of approach developed by Nykänen et al. for welded joints [8–10].

The method can be described by means of Fig. 12 and the following steps:

a. Calculation of real stress and strain values (σ_1, ε_1) referring to the maximum loading

$$\left.\begin{aligned}\varepsilon_1\cdot\sigma_1 &= \frac{\left(K_{f\mathrm{mod}}\cdot\sigma_{\mathrm{nom,max}} + \sigma_r\right)^2}{E}\\\varepsilon_1 &= \frac{\sigma_1}{E} + \left(\frac{\sigma_1}{K'}\right)^{1/n'}\end{aligned}\right\}\rightarrow output\ \ \sigma_1\ \ and\ \ \varepsilon_1\ (4)$$

where $\sigma_{\mathrm{nom,max}}$ is the maximum nominal stress, σ_r is residual stress, E is Young's modulus, n' is the cyclic strain hardening exponent, and K' is the cyclic strength coefficient. $K_{f\mathrm{mod}}$ is a notch-sensitive factor that takes into account the effect of surface quality by means of $C_{\sigma R}$, see example (5), where $C_{\sigma,R}$ is the roughness correction factor for axial stress.

Table 3 Test matrix

Material	T [mm]	N_{sample} [pcs]	R [−]	Manufacturing method
S235	10	5	0	Laser cutting
	10	10	0	Plasma cutting
	10	11	0	Laser cutting + machining
S355	10	10	0	Laser cutting
	10	11	0	Plasma cutting
	10	8	0.4	Plasma cutting
	10	8	0	Plasma cutting + annealing
	10	7	0.4	Plasma cutting + annealing
	10	8	0	Laser cutting + machining
	10	8	0.4	Laser cutting + machining
S960 QC	8	14	0	Laser cutting
	8	8	0	Plasma cutting
	8	8	0.4	Plasma cutting

Fig. 7 Local corner geometry of S960 specimens depending on the cutting process, in practice (**a**–**d**) and schematically (**e**–**f**)
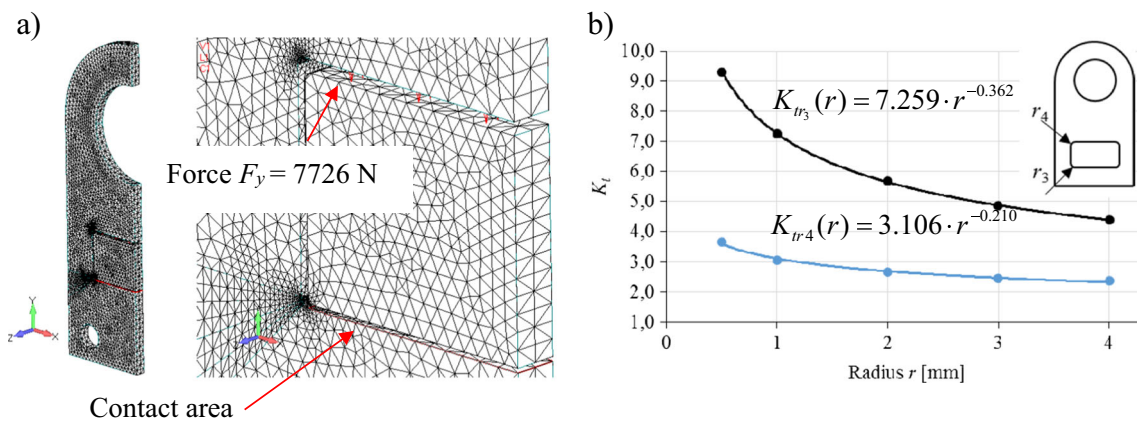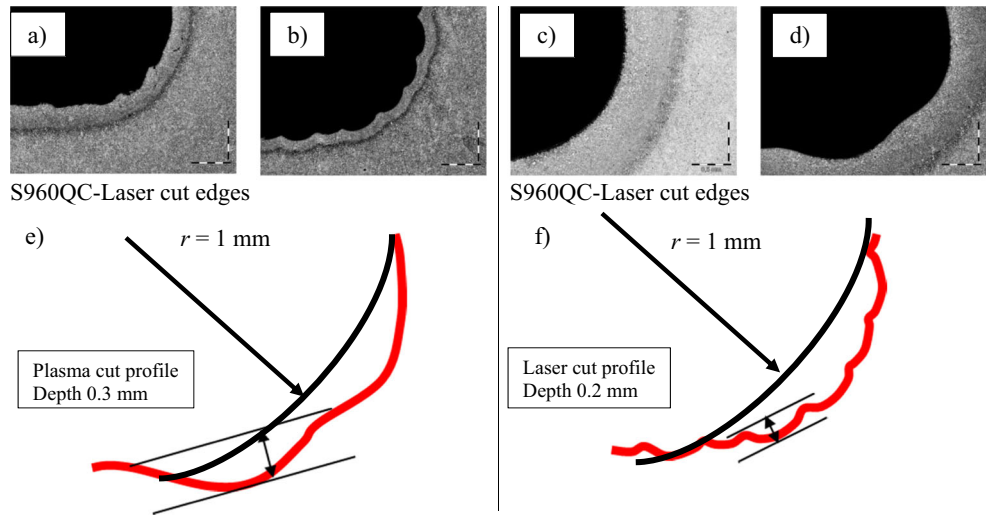
a)   b)   c)   d)

S960QC-Laser cut edges   S960QC-Laser cut edges

e) $r = 1$ mm   f) $r = 1$ mm

Plasma cut profile Depth 0.3 mm   Laser cut profile Depth 0.2 mm

a)   b)

Force $F_y = 7726$ N

Contact area

$K_{tr_3}(r) = 7.259 \cdot r^{-0.362}$

$K_{tr_4}(r) = 3.106 \cdot r^{-0.210}$

Radius r [mm]

Fig. 8 a, **b** FEA model with contact between specimen and wedge, and the stress concentration versus corner radius

$r_3 = 1$ mm   0.3 mm   0.2 mm

488 MPa   100 MPa   735 MPa   806 MPa

Ideal shape   Plasma cut profile   Laser cut profile
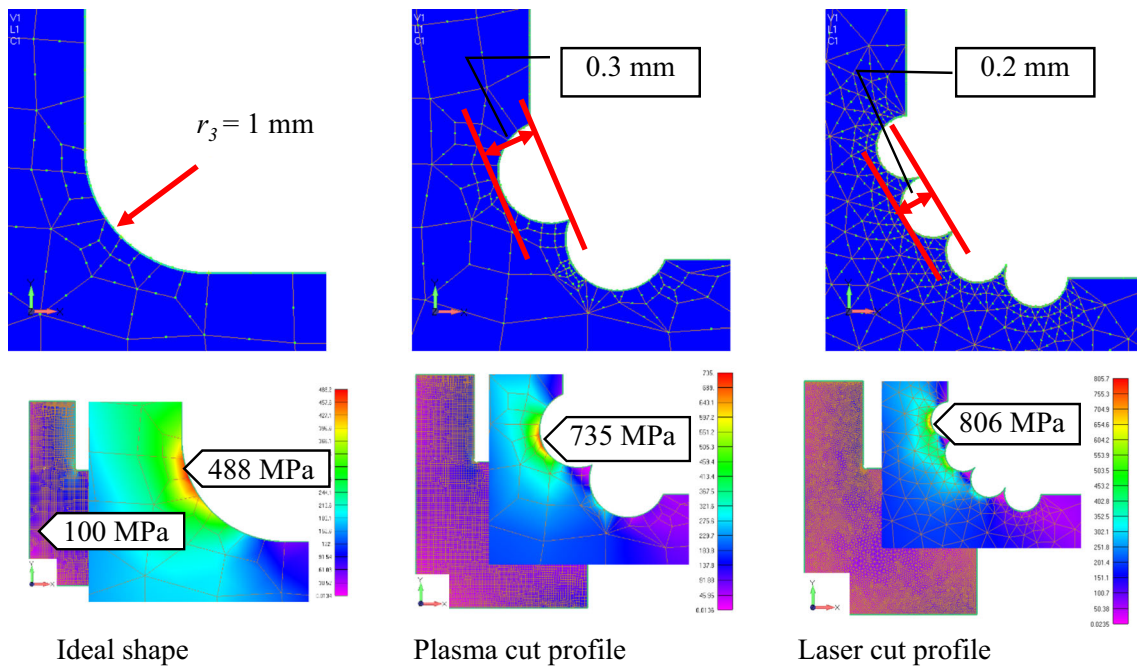
Fig. 9 Effect of local corner geometry on stress concentration
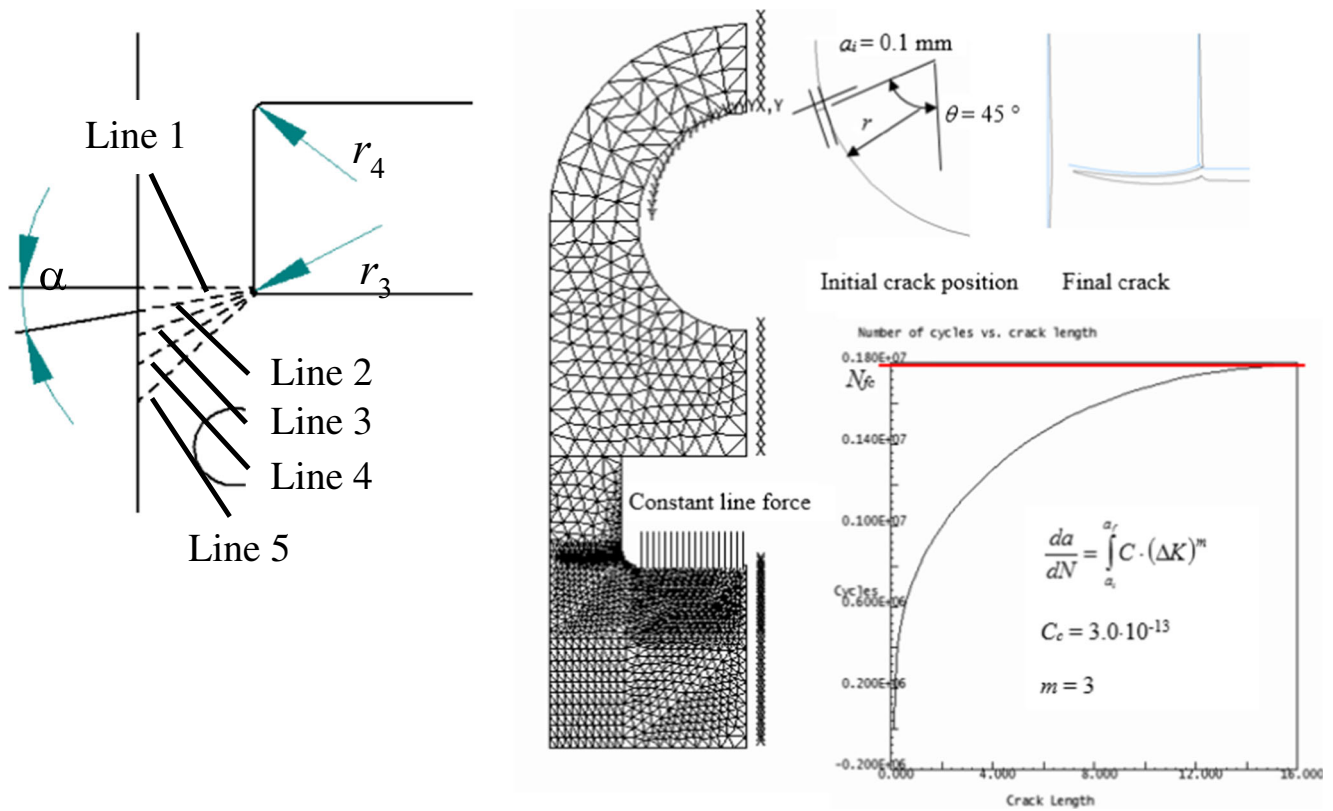
Fig. 10 Potential stress distribution lines for definition of hot spot stress and mesh for LEFM analyses

b. Calculation of modified stress concentration factor ($K_{t,mod}$) taking into account the surface quality

$$K_{f\,\mathrm{mod}} = \left(K_f + \frac{1}{C_{\sigma R}} - 1\right) \qquad (5)$$

$$C_{\sigma,R} = 1 - a_R \cdot \log(R_z) \cdot \log\left(\frac{2 \cdot f_u}{S_{u,min}}\right) \qquad (6)$$

where a_R is a roughness constant (for steel a_R is 0.22), $S_{u,min}$ is minimum ultimate tensile strength (for steel $S_{u,min}$ is 400 MPa), R_z is the roughness value of the surface in [μm], and f_u is the ultimate strength of the material.

c. Calculation of stress and strain ranges ($\Delta\sigma$, $\Delta\varepsilon$) based on Neuber's rule

Fig. 11 Commonly used FAT classes as a function of material yield strength. Range means the quality of the edge according to EN ISO 9013:2002
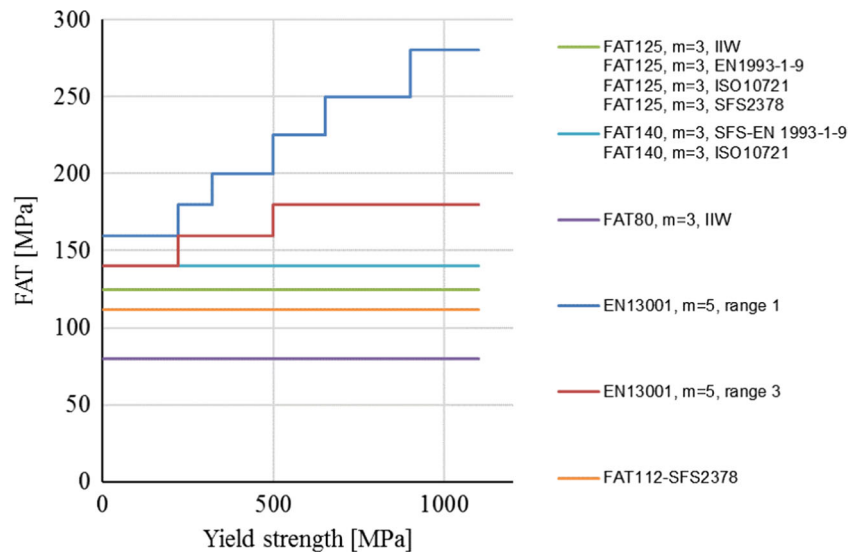
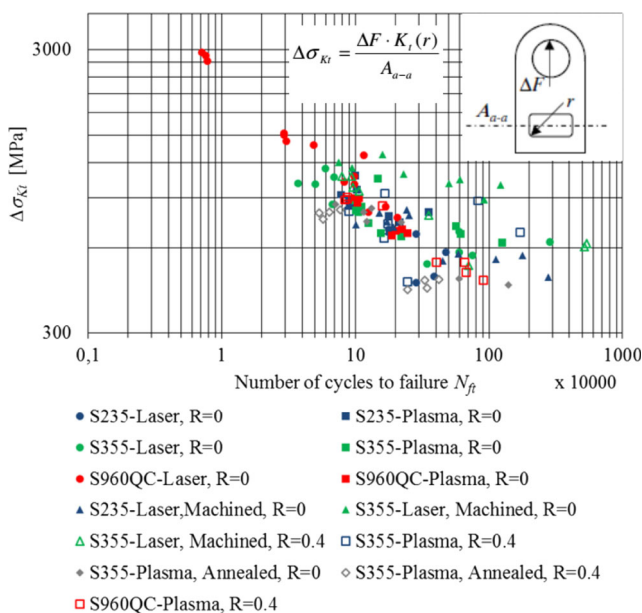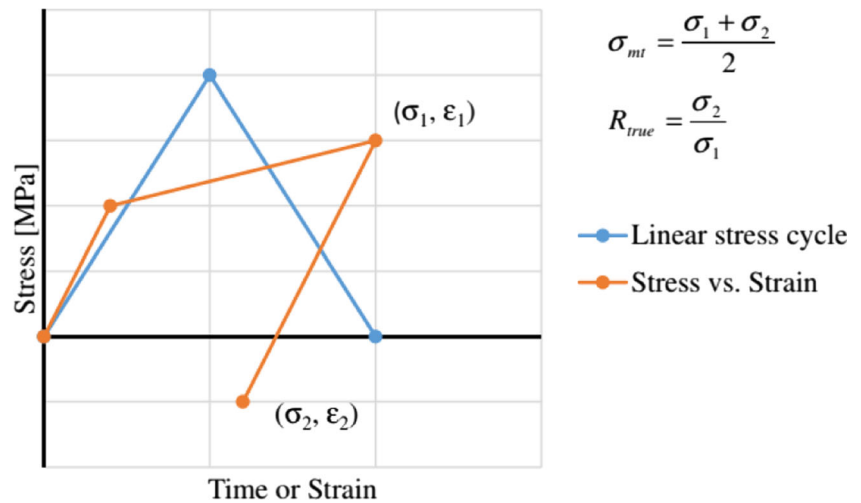**Fig. 12** Definition of true stress ratio

$$\sigma_{mt} = \frac{\sigma_1 + \sigma_2}{2}$$

$$R_{true} = \frac{\sigma_2}{\sigma_1}$$

$$\left.\begin{aligned} \Delta\varepsilon \cdot \Delta\sigma &= \frac{\left(K_{f\,\mathrm{mod}} \cdot \Delta\sigma_{\mathrm{nom}}\right)^2}{E} \\ \Delta\varepsilon &= \frac{\Delta\sigma}{E} + 2\left(\frac{\Delta\sigma}{2\cdot K'}\right)^{1/n'} \end{aligned}\right\} \rightarrow output\ \Delta\sigma\ and\ \Delta\varepsilon \quad (7)$$

where $\Delta\sigma_{\mathrm{nom}}$ is the nominal stress range, $\Delta\sigma$ is the stress range, and $\Delta\varepsilon$ is strain range at the dimensioning detail.

d. Calculation of second stress turn point σ_1 and true stress ratio R_{true}

$$\left.\begin{aligned} \sigma_2 &= \sigma_1 - \Delta\sigma \\ R_{true} &= \frac{\min(\sigma_1, \sigma_2)}{\max(\sigma_1, \sigma_2)} \end{aligned}\right\} \rightarrow output\ \sigma_2\ and\ \ R_{true} \quad (8)$$
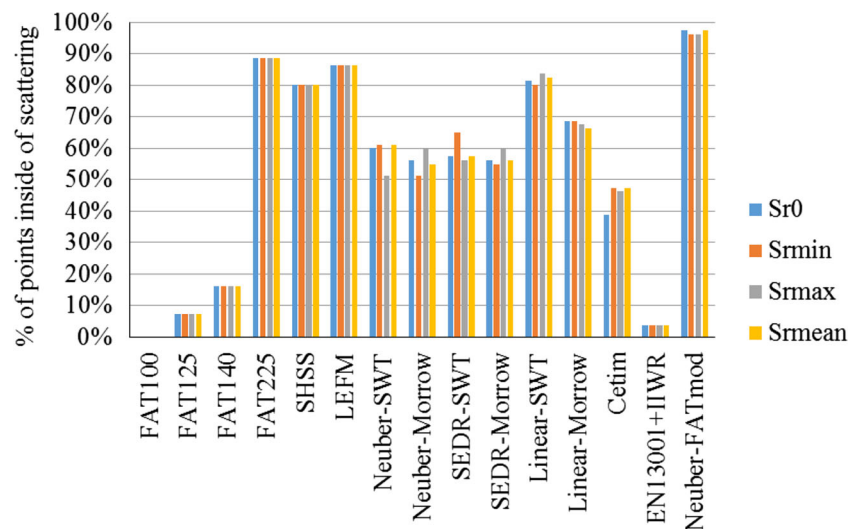
Fig. 13 Experimental results

Fig. 14 The matching between theoretical capacities and experimental test results for cut edges. A probability of 95% is used. Sr0 is the results with a zero residual stress assumption, Srmin with the minimum residual stress assumption, Srmax with the maximum residual stress assumption, and Srmean with the mean residual stress assumption

Fig. 15 Typical failure of the test specimen

e. Calculation of number of cycles $N_{f,\mathrm{mod}}$ with "FAT-mod" method based on nominal stress range

$$N_{f\mathrm{mod}} = \left(\frac{FAT_{m,Rture,ref=0}\cdot\sqrt{1-R_{true}}}{K_{f\mathrm{mod}}\cdot\Delta\sigma_{\mathrm{nom}}} \right)^3 \cdot 2\cdot 10^6 \qquad (9)$$

3 Results

The experimental results are shown in Fig. 13, taking into account the stress concentration in the corner.

Figure 14 presents a comparison between different analysis methods and their variations. The diagram presents the matchings between theoretical values and the experimental results. Four residual stress assumptions have been used in fatigue life calculations. The minimum, maximum, and mean values have been selected from residual stress measurement results [5]. All calculations have also been performed using a zero residual stress assumption.
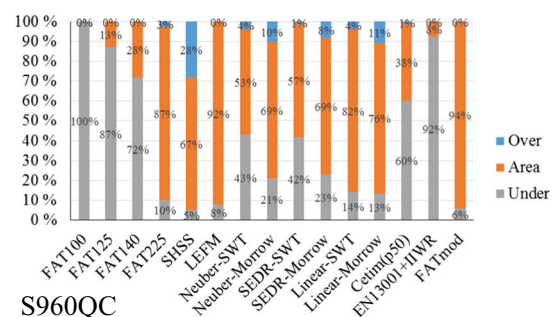
4 Discussion

The critical place of the specimen was the lower corners, and failure occurred there as seen in Fig. 15. The failure patch matches the LEFM estimation seen in Fig. 10 well.
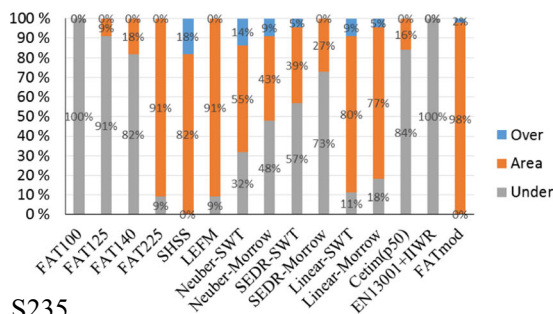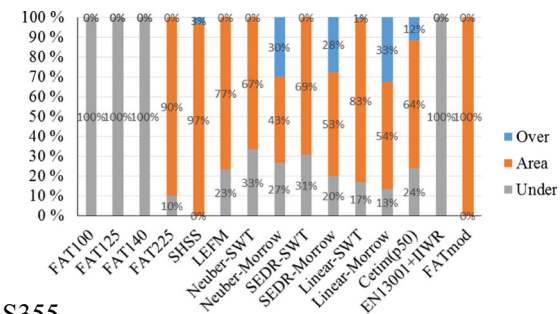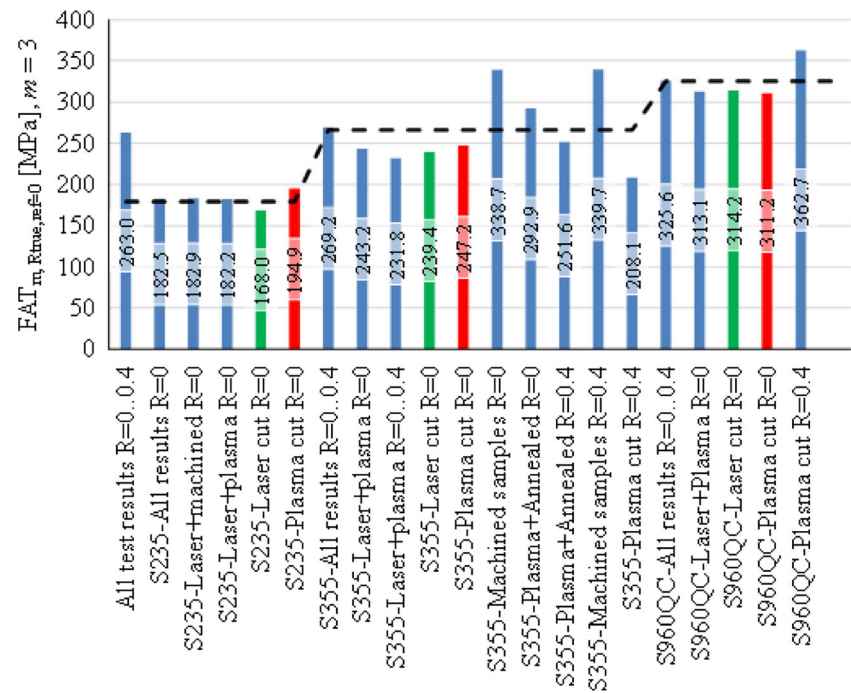

Fig. 16 Average percentage distribution of fatigue strength for tested steel grades

Fig. 17 The fatigue strength depends on the steel grade, cutting method, and stress ratio

The new "FAT-mod" method proved to obtain the best results as shown in Fig. 16. The figure illustrates separately for each steel grade whether the theoretical method will underestimate or overestimate the proven experimental capacities.

The conclusions about quality in terms of the fatigue strength achieved by different cutting processes with a combination of steel grades and stress ratio are illustrated in Fig. 17.

The "FAT-mod" method achieves good results, and the method will be validated for other materials and cutting methods (water-jet cutting) and also for different loading conditions (variable amplitude loading and the effect of overloading).

5 Conclusions

Based on several experimental tests and theoretical calculations, the following conclusions can be drawn:

- The higher the steel grade, the better fatigue resistance of the cut edge
- Residual stress or high external mean stress has an important role in fatigue strength
- Plasma cutting seems to obtain quite the same level of fatigue strengths as machined edges and better fatigue results than laser cutting (due to larger corner radiuses)
- The "FAT-mod" method obtains the best theoretical result

- The "FAT-mod" method and its counter partner, the "3R" method for welded joints, will be extended to new applications in the near future

References

1. Eurocode EN (2005) 1-9 SFS-EN 1993-1-9, Eurocode 3: Design of steel structures. Part 1–9: Fatigue, Helsinki: SFS Finnish Standards Association

2. SFS-EN 13001-3-1:2012 Cranes - General design. Part 3-1: Limit states and proof compentence of steel structure. SFS Finnish Standards Association.

3. Hobbacher A. Recommendations for fatigue design of welded joints and components. IIW document XIII-1965-03/XV-1127-03

4. ISO 10721-1 (1997) Steel structures - Part 1: Materials and design, 1st edn. ISO International Organization for Standardization.

5. Peippo J (2015) A modified nominal stress method for fatigue assessment of steel plates with thermally cut edges. Acta Universitatis Lappeenranta 684. ISNB 978-952-265-905-7 and ISBN 978-952-265-906-4 (PDF)

6. Peterson RE (1973) Stress concentration factors, John Wiley & Sons. ISBN 0-471-68329-9

7. Koh S (1991) Mean stress effects on low cycle fatigue for a high strength steel. Fatigue Fract Engng Mater Struct 14(4):413–428. https://doi.org/10.1111/j.1460-2695.1991.tb00672.x

8. Nykänen T, Björk T (2015) A new proposal for the assessment of fatigue strength of steel butt-welded joints improved by peening. 12

pp. IIW International Conference, High-Strength Materials - Challenges and Applications 2–3 July 2015, Helsinki, Finland

9. Nykänen T, Björk T (2015) Assessment of fatigue strength of steel butt-welded joints in as-welded condition—alternative approach for curve fitting and mean stress effect analysis. Mar Struct 44:288–310. https://doi.org/10.1016/j.marstruc.2015.09.005

10. Nykänen T, Björk T (2015) A new proposal for assessment of the fatigue strength of steel butt-welded joints improved by peening (HFMI) under constant amplitude tensile loading, *Fatigue and Fracture of Engineering Materials and Structures*, 00, pp. 1–17. doi:https://doi.org/10.1111/ffe.12377